ELSEVIER

Journal of Photochemistry and Photobiology A: Chemistry 134 (2000) 127–132

Journal of Photochemistry and Photobiology A:Chemistry

www.elsevier.nl/locate/jphotochem

Rotational level dependence in the collisional removal of CH/D($A^2\Delta$)

Carolina Cerezo, Margarita Martín*

Instituto de Química Física 'Rocasolano',C.S.I.C, Serrano 119, 28006 Madrid, Spain

Received 3 February 2000; received in revised form 3 March 2000; accepted 6 March 2000

Abstract

The dependence on rotational level excitation of the cross sections for removal of CH($A^2\Delta$, v=0) (and the deuterated substitute CD) by CO is measured. Cross sections are found to decrease with increasing rotational level energy. The removal cross sections of the excited CH radical take values that decrease from 6.1 to 1.3 Å^2 for the rotational levels N=4 and 17, respectively. The quenching cross sections of CD($A^2\Delta$, v=0) by CO have slightly smaller values. Quenching cross sections of CH($A^2\Delta$, v=0) by H_2 and Xe have similar dependencies on rotational energy than those observed for the deuterated radical. The rotationally averaged cross sections for CO are about twice larger than for Xe and nearly one order of magnitude larger than for H_2.

Keywords: CH/D($A^2\Delta$); Cross section; Electronic quenching

1. Introduction

Experimental and theoretical studies on the deactivation of the $A^2\Delta$ state of the CH radical with several collision partners, indicate that the mechanisms governing the quenching processes cannot be fitted within the simple models involving long range anisotropic attractive interactions, that have been shown to control the quenching of other excited diatomic hydrides [1–4]. Recent work has provided information about the temperature dependence of the deactivation rate constants of CH($A^2\Delta$) with several small molecules [5,6] and with larger polyatomic quenchers [7]. For most of the collision partners studied, the temperature dependencies are consistent with the presence of an activation barrier in the potential energy surface, although at least in the case of the small molecular quenchers, a simple model based on the formation of a collision complex, modified by an activation energy was unable to represent the temperature dependencies in the high temperature ranges [6].

Previous work carried out in our laboratory has focussed on the quenching dependence on rotational level energy [8–11]. Deactivation cross sections, were measured for several rotational levels of the deuterated radical CD($A^2\Delta$) with CD_2CO (deuterated ketene), H_2 and Xe. Different rotational dependencies were found for each quencher. In the case of hydrogen, although exothermal reaction channels are energetically available, the results were compatible with the presence of a repulsive barrier in the potential energy surface. These results are also qualitatively consistent with the rise of quenching cross section with temperature obtained for the same process [5]. With Xe, cross sections were found to increase with rotational energy for the low rotational levels and to decrease at higher levels, suggesting that a more complex quenching mechanism is involved [11].

Aiming at studying the effect of a collision partner that could form a strongly coupled intermediate with CH/D($A^2\Delta$), in this work we have selected CO as the quencher. Studies on the lower lying excited electronic state of methylidyne, indicate that the quenching by CO proceeds via an intermediate strongly bound collision complex involving several states of the stable CHCO radical [12–14]. Besides the latter, as isotope effects can provide some distinction between different deactivation mechanisms [15], in the present work, we have measured the rotational dependence of the removal rate constants of CH($A^2\Delta$) with H_2 and Xe, in order to compare the results with those previously measured for the deuterated radical [10,11].

2. Experimental section

The experimental set up has been described in previous work [9]. Methylidyne radical in the electronically excited $A^2\Delta$ state was produced in the ArF laser multiphoton dissociation of ketene at 193 nm. Premixed samples

* Corresponding author.
E-mail address: mmm@iqfr.csic.es (M. Martín)

1010-6030/00/$ – see front matter
PII: S1010-6030(00)00259-8

containing fixed pressures of ketene and Ar (typically 0.1 and 15 Torr, respectively) and variable pressures of the quencher gas (in the range 0–1.5 Torr), were photolyzed by the focussed output of the laser, in a glass cell equipped with quartz windows. The fluorescence emission at right angles to the exciting laser beam was monochromated and detected by a photomultiplier. The spectral resolution of the monochromator was appropriated to isolate the emission originating in discrete selected rotational levels of the $A^2\Delta$, v=0 state. The time resolved photomultiplier signals, were recorded by an oscilloscope (Tektronix 2430, 12 ns rise time, 50 Ω loading resistance, 8 bits vertical resolution); typically 256 traces were averaged before being transferred to a microcomputer. Pressures were measured by capacitive manometers Baratron MKS.

Ketene was obtained by pyrolysis of acetic anhydride at 500°C and purified by trap to trap distillation from −107 to −196°C. The deuterated substituted ketene was obained from deuterated acetic anhydride (Cambridge Isotope Laboratories D6, 98%).

Ar (SEO 99.995%), H_2 (Air Liquide 99.995%), CO (UCAR 99.997%) and Xe (UCAR 99.995%) were used without further purification.

3. Results and analysis

3.1. Rotational relaxation effects induced by the quencher

The experimental proceeding followed in this work analyzes the emission starting from a broad population distribution of rotational levels in CD/H($A^2\Delta$), formed in the photolysis of the parent molecule; then, the emission from each rotational level is spectrally isolated and the time resolved traces recorded at different pressures of the quencher are analyzed by the Stern–Volmer method to obtain quenching rate constants. A difficulty associated to this procedure is that the time resolved fluorescence from a given rotational level carries the contribution from electronic (or reactive) removal and rotational energy transfer induced by the quencher. To deconvolute the above effects, the experiments were carried out in the presence of excess of Ar as a buffer gas. Under these conditions, the time evolution of P_N can be written as

$$-\frac{\mathrm{d}P_N}{\mathrm{d}t} = \left(\frac{1}{\tau_{\mathrm{rk}}} + k_N Q\right) P_N + \left(\sum_{N\neq M} k_{N\to M}\mathrm{Ar} + \sum_{N\neq M} k'_{N\to M} Q\right) P_N - \left(\sum_{M\neq N} k_{M\to N}\mathrm{Ar} + \sum_{M\neq N} k'_{M\to N} Q\right) P_M \quad (1)$$

where P_N, Q and Ar are the population densities of the rotational level N, quencher and buffer gas, respectively. $1/\tau_{\mathrm{rk}}$ includes the contribution of radiative lifetime and electronic quenching due to collisions with the parent molecule. k_N is the rate constant for electronic quenching from a given rotational level. $k_{N\neq M}$, $k'_{N\neq M}$, $k_{M\neq N}$ and $k'_{M\neq N}$ are the rate constants for rotational energy transfer between two rotational levels N and M. Electronic quenching by Ar was assumed to be negligible.

Assuming that the rate constants for rotational relaxation by Ar and quencher can be fitted to an exponential gap law model with upwards and downwards transitions related by detailed balance and considering for simplicity only ΔN=±1 transitions, the expression given above can be written as [16]

$$-\frac{1}{P_N}\frac{\mathrm{d}P_N}{\mathrm{d}t} = \frac{1}{\tau_{\mathrm{rk}}} + K_{\mathrm{rot}}(t, Q) + k_Q Q \quad (2)$$

where $K_{\mathrm{rot}}(t, Q)$ is a function that includes the rotational relaxation rates induced by the buffer gas Ar and by the quencher [16]

$$K_{\mathrm{rot}}(t, Q) = k_{N\to N-1}\mathrm{Ar}\left[(1+\alpha) - \beta\frac{P_{N+1}}{P_N} - \gamma\frac{P_{N-1}}{P_N}\right] + k'_{N\to N-1} Q\left[(1+\alpha') - \beta'\frac{P_{N+1}}{P_N} - \gamma\frac{P_{N-1}}{P_N}\right] \quad (3)$$

where $k_{N\neq N-1}$ and $k'_{N\neq N-1}$ are the rate constants for rotational energy transfer between the N and $N-1$ rotational levels; P_M/P_N are the time dependent ratios between the populations of adjacent rotational levels. The coefficients α, β and γ depend on the rotational constants and on the rotational quantum number of the excited radical CH/CD and the former two also depend on the exponential factor appearing in the expression of the rotational rate constants within the exponential gap law model [16].

The expression (2) can be assimilated to the Stern–Volmer equation under certain conditions that render the term $K_{\mathrm{rot}}(t, Q)$ nearly independent on time and quencher pressure. If quencher pressures are kept to values 10 times lower than the pressure of Ar, in the expression of $K_{\mathrm{rot}}(t, Q)$ the term dependent on quencher pressure can be neglected, unless the rotational relaxation rates induced by the quencher were unreasonably fast. Regarding the dependence on time, this is carried by the ratios P_M/P_N between pairs of adjacent rotational levels; if quenching rates vary only smoothly between adjacent rotational levels, the respective populations should decay with not too different total effective decay lifetimes, therefore leading to population ratios that are nearly time independent during a certain time interval. The latter condition is better fulfilled for the high rotational levels; in these, rotational relaxation is much less efficient and so is the population transfer from adjacent levels resulting in fluorescence decays that are close to single exponential functions.

From the above discussion we conclude that the analysis of the exponential portion of the time resolved fluorescence decays can provide values of the quenching rate constants within a reasonable degree of approximation.

3.2. Stern–Volmer analysis of the experimental time resolved fluorescence

The lifetimes of the exponential part of the time resolved decay emissions were measured at different pressures of the quenchers. Linear plots of the reciprocal of the effective lifetimes versus quencher pressure were obtained. Typical plots are shown in Figs. 1 and 2. The rate constants obtained from the slopes of the straight lines, for several rotational levels of CD($A^2\Delta$, v=0) with CO as the quencher, are listed in Table 1. The quenching rate constants for CH($A^2\Delta$, v=0) with H_2, Xe and CO, are listed in Table 2. These rate constants can be compared with the rotationally averaged values reported in the literature; assuming that the rotational distribution in the presence of Ar is not far from Boltzmann rotational equilibrium at 300 K, the rate constants given in Table 2 can be averaged over the rotational population distribution; the averaged values obtained are 5.2×10^{-11} and 0.94×10^{-11} for quenching of CH($A^2\Delta$) with CO and H_2, respectively, in good agreement with values preciously reported in the literature [3].

In order to have some estimation of the errors introduced in the quenching rate constants obtained through the Stern–Volmer method followed here, we have solved numerically the set of coupled differential equations given by Eq. (1). The values of $1/\tau_{rk}$, rotational rate constants by Ar and the initial rotational population distribution in CD($A^2\Delta$, v'=0) were taken from previous work [16]. Regarding the rates for rotational relaxation with the quencher CO, values as high as three times larger than the corresponding values measured with Ar [16] were considered in the kinetic model calculations, therefore allowing the study of the rotational relaxation effects induced by the quencher under highly unfavourable conditions. Vibrational energy transfer from v'=1 to 2 was assumed to have a negligible effect during the lifetime of the emissions similarly to observe for other diatomic hydrides where vibrational relaxation rates have been found to be more than one order of magnitude slower than rotational quenching [17]. The input values of k_N, the rate constants for electronic quenching, were those measured in this work, listed in Table 1. The set of differential equations was

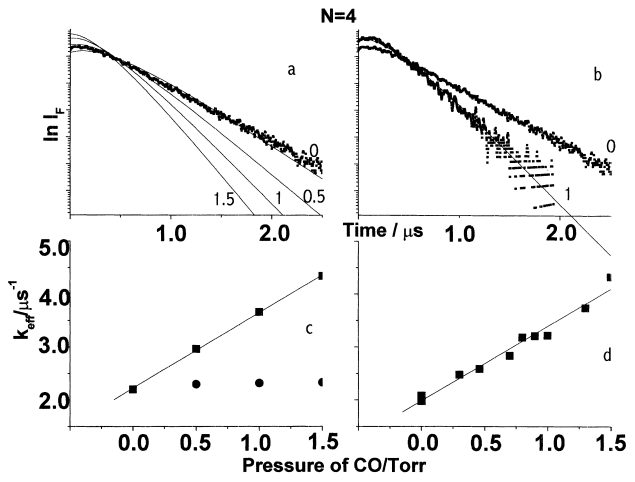

Fig. 1. Semilogarithmic plot of the decay traces for the rotational level N=4, obtained in the ArF photolysis of 0.1 Torr of ketene-d_2, 15 Torr of Ar and CO. Dotted lines are the experimental traces obtained at pressures of 0 and 1 Torr of CO. Continuous lines are the result of the kinetic model calculations described in the text for pressures of CO of 0, 0.5, 1 and 1.5 Torr. In (a) and (b), some of the experimental and calculated traces are superimposed to allow comparison. In (c) and (d), calculated and experimental Stern–Volmer plots obtained representing the effective decay lifetimes measured from the analysis of the decay traces, some of them represented in (a) and (b). Full circles in (c) are the calculated effective lifetimes obtained from the kinetic model calculations when only rotational energy transfer by Ar and CO are included in the model.

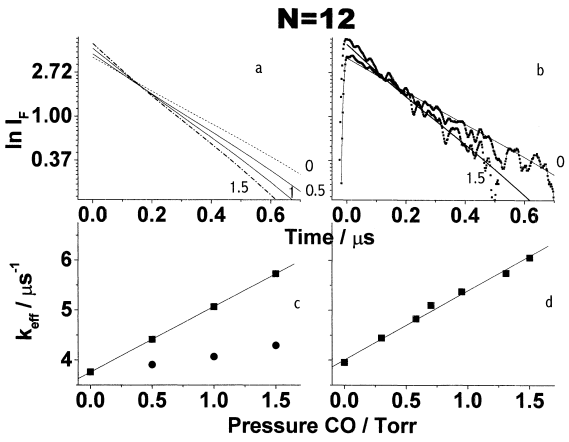

Fig. 2. Semilogarithmic plot of the decay traces for the rotational level N=12, obtained in the ArF photolysis of 0.1 Torr of ketene-d_2, 15 Torr of Ar and CO. Dotted lines are the experimental traces obtained at pressures of 0 and 1 Torr of CO. Continuous lines are the result of the kinetic model calculations described in the text for pressures of CO of 0, 0.5, 1 and 1.5 Torr. In (a) and (b), some of the experimental and calculated traces are superimposed to allow comparison. In (c) and (d), calculated and experimental Stern–Volmer plots obtained representing the effective decay lifetimes measured from the analysis of the decay traces, some of them represented in (a) and (b). Full circles in (c) are the calculated effective lifetimes obtained from the kinetic model calculations when only rotational energy transfer by Ar and CO are included in the model.

Table 1
Removal rate constants for disappearance of CD($A^2\Delta$, v=0) in the presence of CO[a]

Rotational line[b]	k_Q (10^{-11} cm^3 per molecule s^{-1})[c]
P (4)	4.3±0.19
P (5)	4.2±0.36
P (7)	3.9±0.14
R (11)	4.1±0.37
R (12)	4.0±0.4
R (14)	3.5±0.3
R (15)	3.4±0.14
R (16)	2.8±0.3
R (18)	2.3±0.24
R (20)	2.1±0.28

[a] Partial pressure of Ar is 15 Torr.
[b] The number in brackets is the rotational labeling of the upper state.
[c] Errors are two standard errors.

Table 2
Removal rate constants for disappearance of CH($A^2\Delta$, v=0) in the presence of H_2, Xe and CO

Rotational line[a]	k_Q (10^{-11}cm^3 per molecule s^{-1})[b]		
	H_2[c]	Xe[c]	CO
P (4)	0.95±0.09	2.1±0.15	5.2±0.45[d]
P (6)	0.97±0.11	2.8±0.15	4.8±0.3[c,d]
P (8)	1.03±0.11	3.1±0.4	4.3±0.16[c]
R (12)	3.21±0.19	3.2±0.3	2.3±0.1[c]
R (14)		1.7±0.12	
R (17)	4.85±0.32	0.95±0.07	1.1±0.04[c]

[a] The number in brackets is the rotational labeling of the upper state.
[b] Errors are two standard errors.
[c] Partial pressure of Ar is 10 Torr.
[d] Partial pressure of Ar is 15 Torr.

numerically integrated using the routine ACUCHEM [18], for fixed pressures of the parent molecule and buffer gas (0.1 and 15 Torr, respectively) and pressures of CO of 0, 0.5, 1 and 1.5 Torr. The output of the kinetic calculations gave the time evolution of each rotational level population. Stern–Volmer analysis of the latter traces was carried out in a similar way as in the experimental traces and the rate constants k_N retrieved from the slopes of the Stern–Volmer plots were compared to the k_N input values (obtained from the Stern–Volmer analysis of the experimental traces).

The results of the kinetic model calculations have been summarized in Figs. 1 and 2. It has been described in previous work [10,11,16] that, in the presence of 10–15 Torr of Ar, the time resolved decay emissions from rotational levels with $N \leq 8$ builds up for about 250 ns after the photolysis pulse and decays at longer times; the decaying portion at times longer than 400 ns can be fitted to a single exponential. For levels with $N \geq 11$ only quasi monoexponential decays are observed. In Figs. 1 and 2, experimental and calculated decay traces of rotational levels N=4 and 12, respectively, belonging to either regime described above are shown. Effective lifetimes obtained from the quasi monoexponential decay intervals for experimental and calculated traces are plotted versus pressure of CO in the same figures. The slope of the Stern–Volmer plot obtained from the calculated traces retrieves within errors smaller than ±15% the input quenching rate constants (obtained from Stern–Volmer analysis of the experimental traces).

4. Discussion

In order to compare the efficiency of the different quenchers, the rate constants k given in Tables 1 and 2 are converted to cross sections by the expression $k=\sigma\langle v\rangle$. The average speed $\langle v\rangle=(8k_BT/\pi\mu)^{1/2}$, is calculated assuming translational equilibrium at room temperature; k_B and μ are, respectively, the Boltzmann constant and the reduced mass of the collision pair. In Fig. 3, the quenching cross sections are plotted versus rotational level energy. Rotational averaged cross sections, obtained averaging the experimental values over a thermal rotational population distribution are depicted in Table 3.

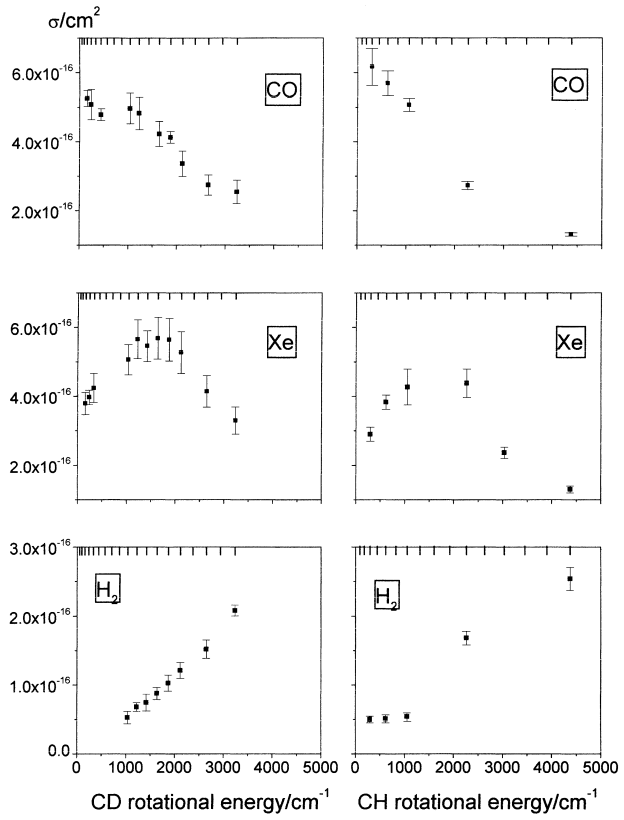

Fig. 3. Cross sections for the quenching of CD/H($A^2\Delta$) in the presence of H_2, Xe and CO.

The cross sections show a different dependence on rotational quantum number for each of the quenchers studied in this work. Quenching of CH($A^2\Delta$) by H_2 and Xe shows a behaviour similar to that previously observed for the deuterated radical. For the low rotational levels, cross sections with H_2 are constant within experimental errors, rising up to a factor of five with increasing rotational energy. Quenching by Xe takes increasing values with increasing rotational quantum number for levels with energy below ~1000 cm^{-1} and decreases for high rotational levels. Quenching of CD($A^2\Delta$) and CH($A^2\Delta$) by CO decreases smoothly with increasing rotational energy. For both CH and CD, at low rotational energies, H_2 is the slowest quencher, with cross sections about a fifth of the values measured for Xe and nearly one order of magnitude slower than for the fastest quencher CO.

The kinetic isotope effect [15], defined as the ratio of rate constants of normal and deuterated radicals, k_{CH}/k_{CD}, is very weak, if any, for quenching by CO; the low rotational levels of CH have slightly faster rate constants than in CD, but the differences can be considered to lie within experimental errors. A weak inverse isotope effect, is observed with Xe; for the latter, quenching of CH is about 80% slower than for the deuterated radical.

Table 3
Experimental cross section measured at the lowest and highest N values of CH and cross sections calculated at the most favourable orientation of the colliders and averaged[a]

Molecule	$\sigma(N_{min})/\sigma(N_{max})$ (Å^2)	σ_{max}/σ_{av} (Å^2)	μ/D	$Q/10^{-21}$ esu cm^2	IP/EV	α (Å^3)	α_{II} (Å^3)	$\alpha_{\perp}$ (Å^3)
CO	6.1/1.3	120/75	0.11[a]	−2.5[c]	14.5[d]	1.95[a]	2.6[b]	1.625[b]
CH(A)			0.88[e]	2.28[f]	8.25[g]	2.2[g]	2.7[g]	2.0[h]

[a] Parameters of the long-range multipolar expansion potential used in the calculation.
[b] See [21].
[c] Taken from Fairchild et al. [22].
[d] See [23].
[e] Refer [24].
[f] See [25].
[g] Taken from Chen et al. [26].
[h] Estimated from the data for a C–H bond in an aliphatic chain, given in [21].

The different rotational level dependence of the rate constants found for each of the quenchers studied in this work, seems to indicate that three different mechanisms are operating. The rotational dependence of cross sections in the quenching by CO indicate an attractive interaction potential. Cross sections calculated assuming that the interaction potential is due to the long range attractive terms of the multipolar expansion are in good agreement with experiment for other diatomic hydrides as OH($A^2\Sigma^+$) and NH($A^3\Pi$). This model does not provide information about cross section dependence on rotational quantum number; however, it has been shown [1,3] that, σ_{max}/σ_{av}, the ratio between the maximum calculated cross section (obtained at the optimum orientation of the colliders) and the value calculated averaging over all possible relative orientations, can be related to $\sigma(N_{min})/\sigma(N_{max})$; $\sigma(N_{min})$ is the experimental cross section obtained for quenching of the excited hydride in the lowest rotational state and $\sigma(N_{max})$ corresponds to the limiting cross section value at high rotational energies. For the pair CH($A^2\Delta$) and CO, calculations within the above model are plotted in Fig. 4, using the multipolar moments and ionization potentials of CO and CH given in Table 3. We obtain that the maximum cross section takes place at the collinear approach of the two molecules; in Table 3, the maximum and averaged cross sections calculated with the model are compared with the experimental values obtained in this work; the calculations lead to a ratio σ_{max}/σ_{av} of 1.6, significantly smaller than the experimental ratio $\sigma(N_{min})/\sigma(N_{max})$.

Cross sections that decrease with rotational quantum number can be obtained in quenching mechanisms proceeding via a strongly bound intermediate complex [19]. The quenching of the low lying $A^4\Sigma^-$ state of CH with CO appears to be driven by the formation of CHCO as the intermediate complex [13,14]; ab initio calculations have provided information about the geometry and well depth of the corresponding intermediate complex and on the location of the relevant portion of the surface of intersection with the lowest $X^2\Pi$ state [13]. Similar calculations would be needed for the higher lying $A^2\Delta$ state in order to asses the participation of the above mechanism and to elucidate the possible participation of ground or excited states of the radical CHCO as the intermediate.

The increasing values of the rate constants with increasing rotational energy, observed in the quenching by H_2, are compatible with the presence of a barrier in the potential energy surface as predicted by theoretical calculations [20] and evidenced by the rate constant dependencies on temperature [6,7]. The presence of a barrier could also provide an explanation for the low rate constants measured in the

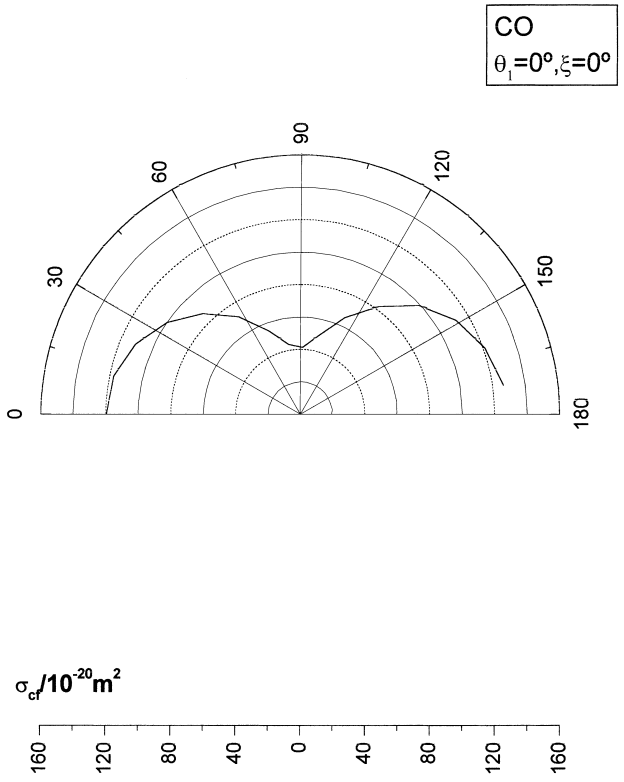

Fig. 4. Multipole forces model. Radial plot of the cross sections for complex formation as a function of the orientation of the molecules CH($A^2\Delta$) and CO. The orientation angles have been defined in [3]. In the inset are given the values of the orientation angles at which the maximum cross section occurs. The parameters of the calculation are listed in Table 3.

quenching of excited methylidyne, more than one order of magnitude slower that for other excited hydrides with the same quencher [1].

In the case of quenching by Xe, the rotational dependence of the rate constants has been discussed in previous work [11]; the present results add not enough evidence to clarify the mechanisms responsible for the bent dependence observed. The rate constants of both isotopic forms are a similar function of the rotational energy, with the maximum values at rotational energies near $1500\,cm^{-1}$, although somewhat slower quenching rates are observed for the protonated mehtylidyne. As the interaction potential between the colliders is expected to be invariant upon isotopic substitution, the kinetic isotopic effect observed may indicate that following the formation of a collision complex, the deuterated substitute could have a larger probability to relaxation into the lower states due to the higher density of states at similar energies.

5. Conclusions

The rotational dependencies of cross sections for removal of $CD(A^2\Delta)$ by CO and the same state of CH by H_2, Xe and CO have been studied. The results indicate that the interaction with H_2 involves the presence of energy barriers in the potential surface; the removal by CO is governed by an attractive potential and a more complicated interaction seems to be present in the quenching by Xe. The nature of the attractive potential in the interaction with CO could be related to the formation as the intermediate of an excited electronic state of the stable radical CHCO.

Acknowledgements

Financial support from Spanish DGESIC (PB96-0844-CO2-01), is acknowledged.

References

[1] R.A. Copeland, M.J. Dyer, D.R. Crosley, J. Chem. Phys. 82 (1985) 4022.
[2] D.R. Crosley, J. Phys. Chem. 93 (1989) 6273.
[3] R.D. Kenner, S. Pfannenberg, P. Heinrinch, F. Sthul, J. Phys. Chem. 95 (1991) 6585.
[4] A.E. Bailey, D.E. Heard, P.H. Paul, M.J. Pilling, J. Chem. Soc., Faraday Trans. 93 (1997) 2915.
[5] P. Heinrich, F. Stuhl, Chem. Phys. 199 (1995) 105.
[6] P. Heinrich, F. Stuhl, Chem. Phys. 199 (1995) 297.
[7] C. Chen, F. Wang, Y. Chen, X. Ma, Chem. Phys. 230 (1998) 317.
[8] J. Luque, J. Ruiz, M. Martin, Laser Chem. 14 (1994) 207.
[9] A. Alonso, M. Ponz, M. Martin, Chem. Phys. Lett. 258 (1996) 465.
[10] M. Martin, M. Castillejo, Chem. Phys. Lett. 266 (1997) 111.
[11] M. Martin, C. Cerezo, Chem. Phys. Lett. 288 (1998) 799.
[12] C.H. Hu, H.F. Schaefer III, Z. Hou, K.D. Bayes, J. Am. Chem. Soc. 115 (1993) 6904.
[13] D.R. Yarkony, J. Phys. Chem. 100 (1996) 17439.
[14] C. Mehlmann, M.J. Frost, D.H. Heard, B.J. Orr, P.J. Nelson, J. Chem. Soc., Faraday Trans. 92 (1996) 2335.
[15] D. Lu, D. Maurice, D.G. Truhlar, J. Am. Chem. Soc. 112 (1990) 6206.
[16] C. Cerezo, R. Torres, J. Ruiz, M. Martin, J. Photochem. Photobiol. A: Chem. 132 (2000) 19.
[17] J.L. Cooper, J.C. Whitehead, J. Chem. Soc., Faraday Trans. 89 (1993) 1287.
[18] W. Braun, J.T. Herron, D. Kahaner, Int. J. Chem. Kinet. 20 (1988) 51.
[19] M. Quack, J. Troe, Ber. Busenges. Physik. Chem. 79 (1975) 170.
[20] A. Vegiri, S. Farantos, Chem. Phys. Lett. 167 (1990) 278.
[21] J.O. Hirscherfelder, C.F. Curtis, R.B. Bird, Molecular Theory of Gases and Liquids, 4th Edition, Wiley, New York, 1967, pp. 440, 947–950.
[22] P.W. Fairchild, G.P. Smith, D.R. Crosley, J. Chem. Phys. 79 (1983) 1795.
[23] Handbook of Chemistry and Physics, 66th Edition, CRC Press, Boca Raton, 1984.
[24] E.A. Scarl, F.W. Dalby, Can. J. Phys. 52 (1974) 1429.
[25] T. Stoecklin, C. Clary, J. Phys. Chem. 96 (1992) 7346.
[26] C. Chen, X. Wang, S. Yu, Q. Lu, X. Ma, Chem. Phys. Lett. 197 (1992) 286.